# On the impact of the plasma jet energy on the product of plasmadynamic synthesis in the Si-C system

**D Nikitin[1] and A Sivkov[1]**
[1]National Research Tomsk Polytechnic University,
634050, Tomsk, Lenin Avenue, 30

E-mail: dima_n@sibmail.com

**Abstract**. Silicon carbide (SiC) nanoparticles can be used for ceramics reinforcement, creation of nanostructured ceramics, microelectromechanical systems. The paper presents the results of plasmadynamic synthesis of silicon carbide nanopowders. This method was realized by the synthesis in an electrodischarge plasma jet generated by a high-current pulsed coaxial magnetoplasma accelerator. Powdered carbon and silicon were used as precursors for the reaction. Four experiments with different energy levels (from 10.0 to 30.0 kJ) were carried out. The synthesized products were analysed by several modern techniques including X-ray diffractometry, scanning and transmission electron microscopy. According to analysis results all the products mainly composed of cubic silicon carbide (b-SiC) with a small amount of unreacted precursors. Silicon carbide particles have a clear crystal structure, a triangular shape and sizes to a few hundred nanometers. Comparison of the results of experiments with different energy levels made it possible to draw conclusions on ways to control product phase composition and dispersion. The silicon carbide content and particles sizes increase with increasing the energy level.

## 1. Introduction

Silicon carbide is the only stable compound in the Si-C system known about hundred years. This material has a combination of different physical and chemical properties as high hardness and mechanical strength, low density, excellent thermal, corrosion radiation resistance, high thermal conductivity [1], [2], [3], [4], [5]. So silicon carbide ceramics is one of the most important non-oxide ceramic materials and it is a very attractive material for a wide range of industrial applications. SiC is a wide band gap semiconductor and it is applied for creation of electronic systems for harsh environments [6], [7], [8]. Nanomaterials are known to have unique and higher properties than conventional materials [9]. Various silicon carbide nanostructures are widely used as ceramics reinforcement, for creation of nanostructured ceramics, micro- and nanoelectromechanical systems (MEMS and NEMS) [10], [11], [12].

The main way of silicon carbide production is the Acheson's process developed in the late of 19th century and still used [13]. It is the carbothermal reduction of silica by coke at 2200–2500 °C. Despite the industrial volumes of the obtained product the Acheson's method has obvious disadvantages as large grain size, long process time and contamination of the product. So this method is not suitable for nanodispersed SiC powders production. There are many successful attempts to synthesize a silicon carbide nanopowder including carbothermal synthesis [14], self-propagating high-temperature process [15], microwave heating method [16], sol-gel process [17], laser synthesis [18] and planetary ball milling [19]. The above synthesis ways have such disadvantages as the high cost, time and energy

expenses and small product volumes. Finding a way of simple and cheap method for the silicon carbide synthesis became the urgent task.

Plasmodynamic method of the nanopowders synthesis is based on the chemical reaction of silicon and carbon in a hypersonic electrodischarge plasma jet. A plasma jet is generated by a high-current pulsed coaxial magnetoplasma accelerator (CMPA). Plasmodynamic method was reported to be used for obtaining nanopowders of materials based on tungsten, silicon and carbon [20], [21], [22].The possibility of silicon carbide synthesis has been shown [22].The present article is devoted to the study of the influence of the energy level on the product characteristics.

## 2. Experimental Conditions

The design of the used experimental installation is shown in Figure 1. The installation consists of a CMPA, a capacitive energy storage and a working chamber. The CMPA includes the central electrode with the graphite insert and the insulator and the graphite accelerator channel. A mixture of amorphous carbon black and micron crystalline silicon powder with the Si:C ratio 3:1 was used as precursors. The averaged sizes of silicon and carbon particles were ~50 μm and ~30 nm, respectively. The precursors mass was ~ 1.0 g. The mixture was placed into the plasma forming zone of accelerating channel. The Si-C mixture also provided the initiation of an arc discharge between the central electrode and the graphite accelerating channel after circuit locking. The CMPA was supplied by the capacitive energy storage with a capacity C = 6 mF. An accumulated energy Wc was changed by varying of the charging voltage Uc from 2.0 kV to 3.5 kV. Four experiments with different voltages were conducted.

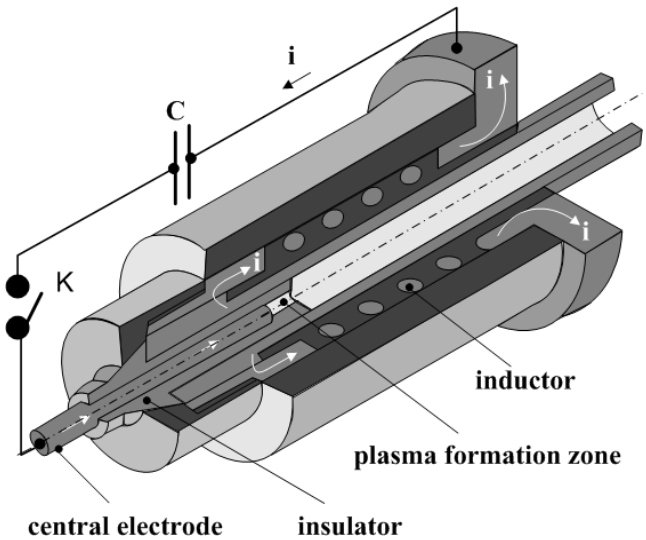


**Figure 1.** Schematic diagram of the coaxial magnetoplasma accelerator.

Typical oscillograms of working current and voltage on electrodes were obtained by a Tektronix TDS1012 oscilloscope. Average values of energy parameters (operating current Im, the voltage on electrodes Um, discharge power Pm and energy W) are shown in Table 1. Plasma shots were produced in a sealed volume of the cylindrical reactor chamber filled with argon at normal pressure and room temperature. The plasma jet impacted on the copper barrier installed at a distance of 23 mm from acceleration channel. The powder synthesized product was collected from the wall of the reactor chamber after precipitation of suspended particles.

Synthesized in the experiments powder products were analyzed without any preparation by such modern methods: X-ray diffraction (XRD) using a Shimadzu XRD 6000 diffractometer (CuKα-radiation, $\lambda$ = 0.15406 nm), transmission electron microscopy (TEM) using Philips CM 12 microscope. Qualitative X-ray analysis was made by PowderCell 2.4 software package using a database PDF4+.

**Table 1.** The average size of nanoparticles and aggregates in suspensions.

| Energy parameters | Experiments | | | |
|---|---|---|---|---|
| | 1 | 2 | 3 | 4 |
| $U_c$ [kV] | 2.0 | 2.5 | 3.0 | 3.5 |
| $I_m$ [kA] | 65 | 76 | 98 | 111 |
| $U_m$ [kV] | 1.0 | 1.1 | 1.3 | 1.8 |
| $P_m$ [MWt] | 65 | 76 | 123 | 204 |
| $W_c$ [kJ] | 12.0 | 18.8 | 27.0 | 36.8 |
| W [kJ] | 10.5 | 13.0 | 19.0 | 29.7 |

## 3. Results and discussion

The XRD-studies of synthesized powders are presented in the form of X-ray diffraction patterns in Figure 2. The results of structural and phase analysis are shown in Table 2. The character of XRD-patterns and the set of different coherent reflections show the practical absence of amorphous component in the synthesis product and demonstrate the presence of several crystalline phases in all cases. According to computer calculations by PowderCell 2.4 software the powder product of plasmodynamic synthesis in all cases consists of four crystalline phases with the following crystallographic parameters of structural models: cubic silicon carbide β-SiC, space group SPGR – F-43m {216}; cubic silicon cSi, SPGR – F-43/d-32/m {227}; graphite gC, SPGR – P6-3mc {186}; carbon onions structure C-Onions, SPGR – P6-3mc {186}. The most intense peaks belong to respective planes (111), (200), (220), (311), (222) of cubic silicon carbide. Results of the comprehensive analysis of the X-ray diffraction pattern of the synthesized products (including phases contents and coherent scattering areas) are presented in Table 2.

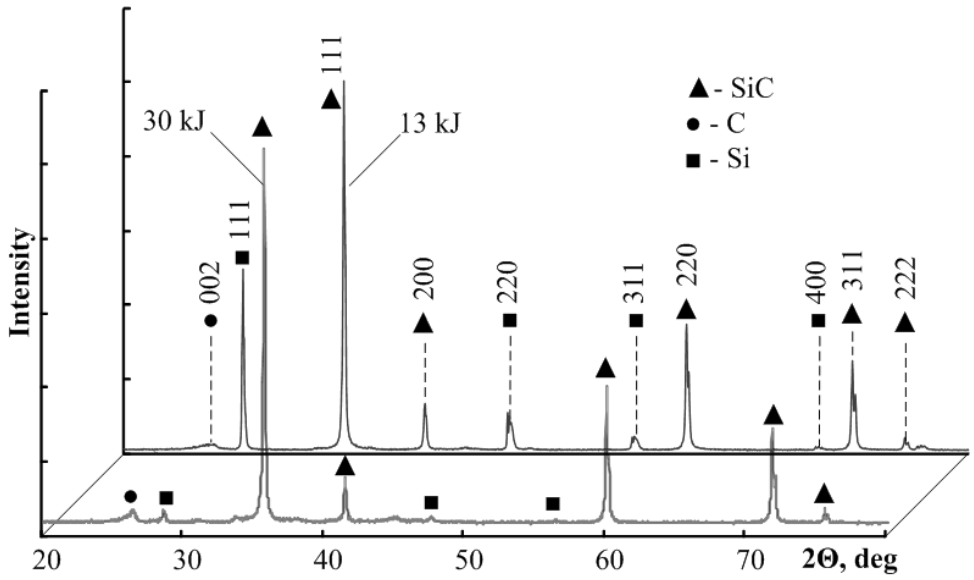


**Figure 2.** Diffraction patterns of the synthesized powders.

According to the calculated data of XRD analysis a cubic phase of silicon carbide has the highest content in the product. More efficient formation of silicon carbide (higher SiC content) is observed at higher values of discharge energy W. The carbon content do not decreases in the range of discharge energy from W = 13.5 to W = 29.7 kJ due to increase of the graphite eroding by the central electrode. The growth of SiC particle sizes is observed with increasing energy in the entire range. The growth of content and particle sizes of silicon carbide can be explained by more fully ionization precursors due to the higher pressure and temperature parameters (pT-parameters). Dependences of the content ω in the product of silicon carbide, silicon and carbon on discharge energy W are shown in Figure 3.

**Table 2.** The average size of nanoparticles and aggregates in suspensions.

| Phase *W* [kJ] | | SiC | Si | C |
|---|---|---|---|---|
| 1. 10.5 | Content [%] | 60.0 | 24.0 | 16.0 |
| | CSA [nm] | 35 | 20 | 10 |
| 2. 13.0 | Content [%] | 73.0 | 19.0 | 8.0 |
| | CSA, [nm] | 70 | 80 | 20 |
| 3. 19.0 | Content [%] | 80.0 | 13.0 | 7.0 |
| | CSA, [nm] | 75 | 65 | 35 |
| 4. 29.7 | Content [%] | 90.0 | 3.5 | 6.5 |
| | CSA, [nm] | 90 | 40 | 20 |

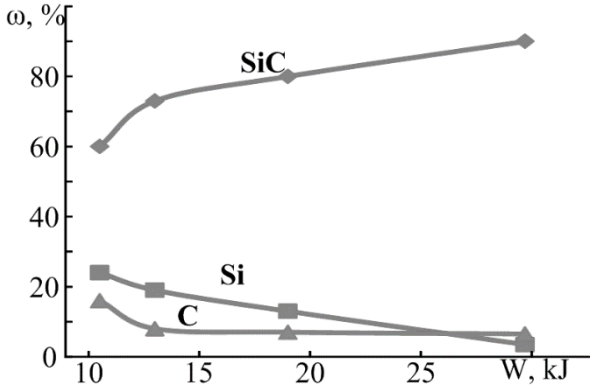


**Figure 3.** Dependences of the content ω in the product of silicon carbide, silicon and carbon on discharge energy W.

Results of the analysis of synthesis product by transmission electron microscopy confirm and complement the XRD data. Bright-field TEM-image of a powder produced at the maximum energy W = 30 kJ is shown in Figure 4. According to the TEM-image the synthesized product consists of two different fractions of particles. The first fraction (1) is represented by particles with close to "ideal" crystallographic design in the shape of triangles with truncated vertices and hexagons of sizes to 400 nm. Such particle shapes is typical for silicon carbide crystals [23]. The selected area electron diffraction (SAED) is presented in Figure 5. The most striking and the main diffraction reflexes relate to reflecting planes of cubic silicon carbide. There are weak-intensive reflections related to the carbon phase.

Dark-field TEM-image of a powder produced at the maximum energy W = 30 kJ is presented in Figure 5. These pictures were obtained at the diffracted light beam on the packets plane SiC (111). The glow of reflecting planes of particles (1) can be seen. It proves the particles of this fraction relate to silicon carbide phase.

Fraction 2 represents particles of size to a few tens of nanometers in the form of amorphous structures and crystalline objects of uncertain morphology. They can be considered as belonging to the phases of the unreacted precursors of silicon and carbon [21].

## 4. Conclusions

Silicon carbide (SiC) nanopowders were produced by plasmadynamic synthesis. This method was realized by the synthesis in an electrodischarge plasma jet generated by a high-current pulsed coaxial magnetoplasma accelerator. Four experiments with different energy levels (from 10.0 to 30.0 kJ) were carried out. The synthesized products were analyzed by several modern techniques including X-ray diffractometry, scanning and transmission electron microscopy. According to analysis results all the products mainly composed of cubic silicon carbide (β-SiC) with a small amount of unreacted

precursors. Silicon carbide particles have a clear crystal structure, a triangular shape and sizes to a few hundred nanometers. Comparison of the results of experiments with different energy levels made it possible to draw conclusions on ways to control product phase composition and dispersion. The silicon carbide content and particles sizes increase with increasing the energy level.

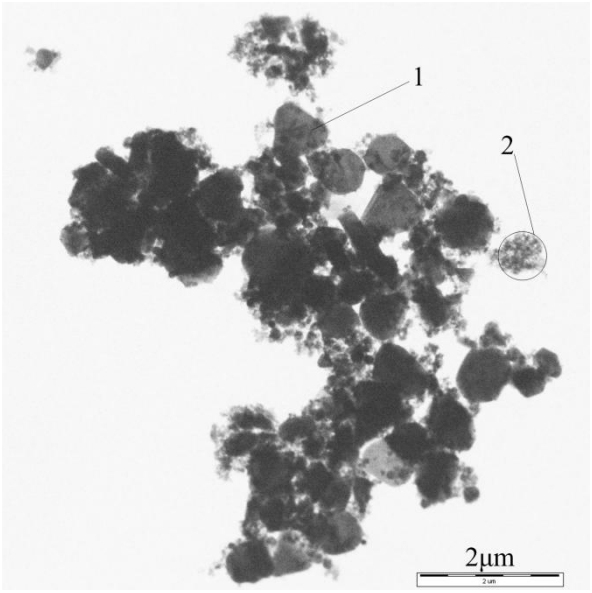


**Figure 4.** Bright-field TEM-images of the plasmadynamic synthesis product (W = 29.7 kJ).

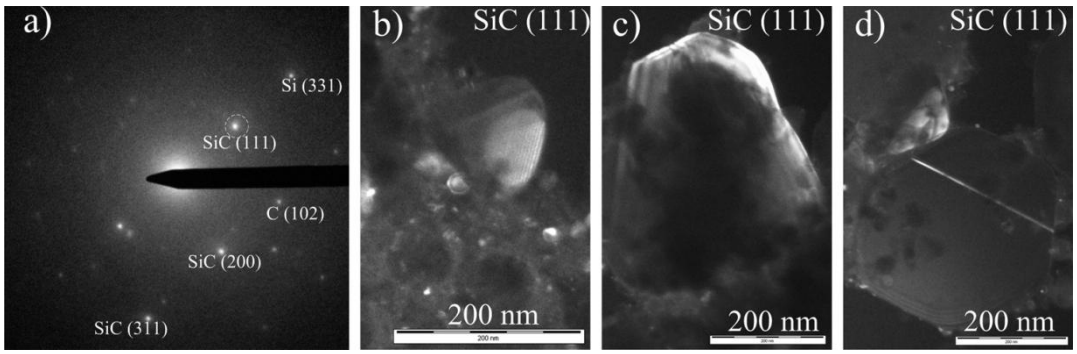


**Figure 5.** TEM-images of the plasmadynamic synthesis product (W = 29.7 kJ): (a) SAED, (b), (c), (d) dark-field images

**Acknowledgments**
This work was supported by the Russian Science Foundation (project no. 15-19-00049).

**References**

[1] Harris G L 1995 *Properties of Silicon Carbide* (London: NSPEC)
[2] Gerhardt R 2011 *Properties and Applications of Silicon Carbide* (Rijeka: InTech)
[3] Sarin V K 2014 *Comprehensive Hard Materials. Volume 2, Ceramics* (Oxford: Elsevier Ltd.)
[4] Watari K 2001 *J. Ceram. Soc. Japan.* **109** S7-S16
[5] Wu R, Zhou K, Yue C Y, Wei J and Pan Y 2015 *Prog. Mater Sci.* **72** 1-60
[6] Chin H S, Cheong K Y and Ismail A B 2010 *Metall. Mater. Trans. B.* **41 4** 824-832
[7] Willander M, Friesel M, Wahab Q and Straumal B 2006 *J. Mater. Sci. - Mater. Electron.* **17** 1-25
[8] Wang Z, Shi X, Tolbert L M, Wang F F, Liang Z, Costinett D and Blalock B J 2015 *IEEE T. Power Electr.* **30 3** 1432-1445

[9] Cao G and Wang Y 2011 *Nanostructures and Nanomaterials: Synthesis, Properties, and Applications*, (Singapore: World Scientific Publishing Co. Pte. Ltd.)
[10] El-Daly A A, Abdelhameed M, Hashish M and Daoush W M 2013 *Mater. Sci. Eng. A.* **559** 384-393
[11] Filipescu M, Stokker-Cheregi F, Colceag D, Nedelcea A, Birjega R, Nistor L C and Dinescu M 2013 *Appl. Surf. Sci.* **278** 96-100
[12] Maboudian R, Carraro C, Senesky D G and Roper CS 2013 *J. Vac. Sci. Technol. A.* **31** 1-18
[13] Acheson G 1893 *Production of artificial crystalline carbonaceous material* U S Patent 492 767.
[14] Rajarao R, Ferreira R, Sadi S H F, Khanna R and Sahajwalla V 2014 *Mater. Lett.* **120** 65-68.
[15] Huczko A, Kurcz M, Dabrowska A, Baranowski P, Bhattarai A and Gierlotka S 2014 *J. Cryst. Growth* **401** 469-473.
[16] Van Laar J H, Slabber J F M, Meyer J P, van der Walt I J, Puts G J and Crouse P L 2015 *Ceram. Int.*, **41 3 B** 4326-4333.
[17] Omidi Z, Ghasemi A and Bakhshi S R 2015 *Ceram. Int.* **41, 4** 5779-5784.
[18] D'Amato R, Falconieri M, Gagliardi S, Popovici E, Serra E, Terranova G and Borsella E 2013 *J. Anal. Appl. Pyrolysis* **104** 461-469.
[19] Abderrazak H and Abdellaoui M 2008 *Mater. Lett.* **62, 23** 3839-3841.
[20] Pak A, Sivkov A, Shanenkov I, Rahmatullin I and Shatrova K 2015 *Int. J. Refract. Met. Hard Mater.* **48** 51-55.
[21] Sivkov A A, Nikitin D S, Pak A Y, Rakhmatullin I A 2013 *J. Superhard Mater.* **35, 3** 137-142.
[22] Sivkov A A, Pak A Y, Nikitin D S, Rakhmatullin I A, Shanenkov I I 2013 *Nanotech. in Rus.* **8** 489-494.
[23] Feng A and Munir Z A 1995 *Metall. Mater. Trans. B.* **26 3** 587-593.